コンクリート工学年次論文報告集, Vol.15, No.2, 1993

論 文

[2211] Computational Model for Steel Bar Embedded in Concrete under Combined Axial Pullout and Transverse Shear Displacement

Juneid QURESHI *1 and Koichi MAEKAWA *2

1. INTRODUCTION

For rational and accurate prediction of the behavior of reinforced concrete structures the understanding and formulation of predictive models for both strength and deformational behavior are needed. At present several constitutive laws exist at the material level, which can be combined to formulate plate and joint models for smeared and discrete crack elements for FEM application, which is one of the powerful tools to predict strength and deformational structural concrete behavior. However these constitutive laws have been verified under simplified and idealized loading conditions, and their applicability under generic conditions need to be checked. The relation between bond stress-slip-strain has been formulated in the past [2] by treating the reinforcement in concrete as a one dimensional cord element. This consideration is valid for a single mode deformational path in which the reinforcement is subjected to axial deformation only. However in reality when deformational paths are of a mixed mode nature, i.e. axial pull-out coupled with transverse shear displacement, as shown in Fig. (1), the applicability of the existing model is invalidated due to the reduction in the axial stiffness and the mean yield strength of the reinforcement, due to a zone of localized curvature in the reinforcement close to the crack plane [1]. This paper attempts to formulate a relationship between the localized shear displacement and the maximum curvature in the reinforcement, thereby proposing an enhanced computational model for the prediction of bar behavior under the generic condition of axial pullout and transverse shear.

2. LITERATURE

The modelling of reinforcement has till now been treatedby most researchers by separately considering the two actions of axial pull-out and transverse shear and then superposing the behavior. In the past predictions for the shear capacity of a crack plane was made by the superposition of bar axial bond stress-strain-slip model [2], with plain concrete stress transfer model [3], to predict shear capacity of RC interfaces. However, the predictions were not satisfactory, usually resulting in over estimation of capacity, even while neglecting dowel contribution by the reinforcement [4]. Since the bond-slip-strain model proposed in [2] was formulated under pure tensile conditions, it was presumed that one of the major reasons for the incorrect estimation of shear capacity is the incorrect model for estimating confinement provided by the axial stiffness and strength of the reinforcement under coupled action of crack opening and transverse shear.

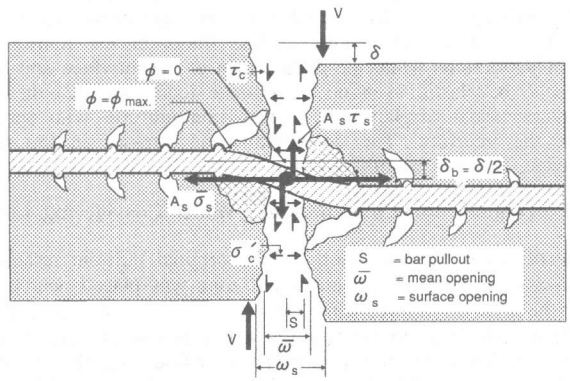

Fig. 1: Embedded bar subjected to coupled displacement path

*1 Graduate Student, The University of Tokyo
*2 Associate Professor, The University of Tokyo

3. PULLOUT TESTS COUPLED WITH TRANSVERSE SHEAR

To investigate the embedded bar behavior under a coupled displacement path, pure shear loading was adopted in beam type specimens, as shown in Fig. (2). The shear displacement and associated dilatancy of the shear plane simulates the necessary generic loading path for the embedded bar. By changing either the confining force to the interface, by varying the reinforcement ratio, or the shear plane geometry, different displacement paths can be studied. Test results showed significant decrease in bar axial stiffness and strength, under the coupled displacement paths. Details of the test setup and results can be found in [1].

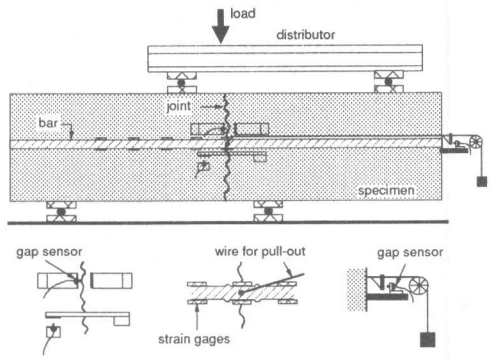

Fig. 2: Experimental set-up

4. ANALYTICAL MODELLING

4.1 REVIEW OF BOND STRESS-STRAIN-AXIAL SLIP MODEL OF EMBEDDED BAR

Shima et al. [2] proposed a bond stress-strain-axial slip model for RC reinforcement under uniaxial pull-out conditions. This model which takes into account effects of bar diameter, concrete strength and embedded length of bar is taken as the framework on which modifications for the proposed model are introduced. The governing equations for this model are,

$$\tau_b = \frac{E_s D}{4}\frac{d\varepsilon}{dx} = \frac{0.73 f_c' [\ln (1 + 5000 S / D)]^3}{1 + 10^5 \varepsilon_s} \quad ; \quad S(x) = \int_0^x \varepsilon_s(x) + S_o \qquad (1)$$

where τ_b is the bond stress, S and S_o are defined as slip relative to the free end and slip of bar at free end, respectively. D is the bar diameter and ε_s is the bar axial strain.

4.2 GENERIC MODEL OF EMBEDDED BAR: BOND STRESS-STRAIN-COUPLED SLIP MODEL

In reference [1], it has been reported that the two new features of bar behavior, which were witnessed experimentally, included (1) the non-uniformity in the distribution of mean strains close to the crack plane, with some extreme fibers in the reinforcement reaching plastic strains at some particular sections while the mean strain at the interface and other points away from the interface were found to be elastic even up to ultimate loads, and (2) the curvature induced in the bar due to the transverse shear displacement is also non uniform with zero curvature at, and some distance away from, the interface. The computed mean stresses in the reinforcement, close to the crack plane, however, showed roughly uniform nature.

4.2.1 Proposals for Computational Model Considering Localized Effects

Zone of Bond Deterioration: In the original pull-out tests carried out to formulate the bond stress-strain-axial slip model, an unbonded zone was placed near the loaded surface to ensure uniform bond over the whole reinforcement. However in reality the bond performance near the interface may easily be deteriorated due to the splitting and crushing of concrete around the bar. In order to consider this effect, a '*Bond Deterioration Zone*' is defined, L_b, the range of which is a function of bar diameter, i.e. $L_b = L_b\ (D)$. For the computational model L_b is taken as '5D'. The degradation for the bond stress, τ_b, along this zone is modelled by a simple bi-linear function, as expressed below,

$$\tau_b\ (x) = \tau_{b,\max} - \frac{\tau_{b,\max}}{L_b}\{x - (L_e - L_b)\} \qquad (L_e - L_b \le x \le L_e - \frac{L_b}{2})$$
$$\tau_b\ (x) = 0 \qquad (L_e - \frac{L_b}{2} \le x \le L_e) \qquad (2)$$

where $\tau_{b,max}$ is the maximum bond stress attained at the origin of L_b. L_e is the bar embedded length.

Zone of Curvature Influence: To consider the effect of the localized curvature in the bar, close to the shear plane, the concept of a '*Curvature Influencing Zone*', L_c, is introduced. In the tests L_c was observed to be between '4*D*' and '5*D*' initially, with a small increase with increasing load. For the model, the initial zone size, L_c ($=L_{co}$), at small displacements when both materials can be considered to behave elastically, is idealized by considering the bar behavior analogous to a beam on an elastic foundation (BEF). L_{co} is taken as three times the size of the location of the maximum bending moment, and consequently of maximum curvature, as would be derived from BEF analogy, to give,

$$L_{co} = \frac{3\pi}{4}\sqrt[4]{\frac{4 E_s I_b}{k D}} \qquad \left(k = \frac{150 f_c'^{0.85}}{D} \right) \tag{3}$$

where k is the foundation modulus for concrete, and E_s and I_b are the elastic modulus and moment of inertia of bar section, respectively. The BEF analogy, however, can not be considered reliable in the later stages of bar pullout and shear displacement, since both the embedded bar and the supporting concrete would be behaving nonlinearly. The gradual softening in the supporting concrete due to increasing bar shear displacements, δ_b, and radial micro bond cracks from bat pullout, S, is modelled by considering an increase in L_c, as a function of L_{co} and a non-dimensional damage build-up parameter, DI, as expressed below,

$$DI = (1+150\ S\ /\ D)\ \delta_b\ /\ D$$
$$L_c = L_{co} \quad (for\ \ DI \le 0.02) \quad ; \quad L_c = L_{co} * \{1+3*(DI-0.02)^{0.85}\} \quad (for DI > 0.02) \tag{4}$$

The variation of L_c has been verified with test results. The shape of the curvature distribution, $\phi(x)$, within L_c is modelled by a skewed parabolic form, as seen in test results, and expressed by

$$\phi\ (x) = \frac{3\ \phi_{max}\ [x - (L_e - L_c)]^2}{L_c^2} \qquad \left(L_e - L_c \le x\ L_e - \frac{L_c}{2}\right)$$
$$\phi\ (x) = -3\ \frac{\phi_{max}}{L_c^2}\ [3\ \{x - (L_e - \frac{L_c}{2})\}^2 - L_c\ \{x - (L_e - \frac{3\ L_c}{4})\}] \qquad \left(L_e - \frac{L_c}{2} \le x \le L_e\right) \tag{5}$$

Using the classical beam theory assumptions, compatibility conditions require that the double integral of the curvature distribution along the bar axis, $\phi(x)$, must equal the displacement of the bar normal to that axis, δ_b, which is one half the shear plane displacement, δ. Satisfying boundary and continuity conditions, and neglecting bar shear deformations, we have

$$\delta_b = \int\int_{L_c} \phi\ (x)\ dx \qquad (\text{where}\ \ \delta_b = \delta\ /\ 2) \tag{6}$$

4.2.2 Stresses, Strains and System of Forces Acting on Embedded Bar Modelled as 2-D Cord

From the assumed distribution profiles of bond stresses and curvature, computations can be carried out for the sectionally averaged mean bar stresses and strains along the bar axis, $\overline{\sigma_s}(x)$ and $\overline{\varepsilon_s}(x)$, respectively, the stresses and strains along the bar cross section, $\sigma_f(y)$ and $\varepsilon_f(y)$, respectively (where y is the local coordinate, the origin of which is the centroid of the section concerned), and the system of forces, including bending moments $M(x)$, shear forces $V(x)$ and contact pressure below the bar $f_b(x)$, along the bar axis. The discretized bar fiber stresses, $\sigma_f(y)$, are computed from the uniaxial stress-strain relationship of bare steel bar [2]. The computational flow is detailed below.

$$\overline{\sigma_s}\ (x) = \frac{4}{D}\int_0^x \tau_b\ (x)\ dx \qquad where \qquad \tau_b\ (x) = \tau_b\ (x, \tau_{b,max}) \qquad (L_e - L_b \le x \le L_e) \tag{7}$$

$$\overline{\varepsilon_s}\ (x) = \overline{\varepsilon_s}\ (\phi\ (x), \overline{\sigma_s}\ (x)) \qquad (L_e - L_b \le x \le L_e) \tag{8}$$

$$where \quad \overline{\sigma_s}\ (x) = \int_{-D/2}^{D/2} \sigma_f\ (\varepsilon_f)\ dA_s\ (y)\ /\ A_s \quad and \quad \varepsilon_f = \overline{\varepsilon_s}(x) + \phi\ (x) * y \tag{9}$$

$$M(x) = \int_{-D/2}^{D/2} \sigma_f\ (\phi(x), y).\ y.\ dA(y) \quad (10) \quad ; \quad V(x) = \frac{dM(x)}{dx} \quad (11) \quad ; \quad f_b(x) = \frac{dV(x)}{dx} * \frac{1}{D} \quad (12)$$

The effect of the shear stress, τ_s, due to the bending curvature, on the yield stress of the bar

is taken into consideration by applying the Von-Mises yield criterion, as below

$$f'_y(x) = f_y \sqrt{1 - 3\,(\tau_s(x) / f_y)^2} \tag{13}$$

by which the reduced mean yield stress, f'_y, for checking the fiber stress state of the bar is obtained. The spatial distribution profile of the computed parameters, along the bar axis, are shown in Fig. (3). Also shown are the profile of fiber stresses across the bar section along the *'Curvature Influencing Zone'*. It is to be noted that the above formulations are not constricted by the pre-yield or post-yield bar behavior, since the basic geometric compatibility between the transverse bar displacement and the curvature holds true irrespective of elastic or plastic material behavior. This increases the versatility of the model to deal with the nonlinear interaction between the bar and surrounding concrete.

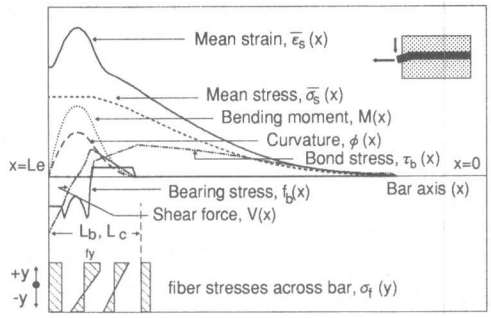

Fig. 3: Distribution profiles of computed parameters

4.2.3 Ultimate Axial Force Criterion for Embedded Bar

The ultimate axial force provided by the reinforcement under a coupled displacement path is defined by the limiting criterion, $\lambda(x)$, for interactive stresses produced due to combined bending moment $M(x)$, shear force, $V(x)$, and axial force, $P(x)$, on the bar, and expressed as

$$\lambda(x) = \left[\frac{M(x)}{M_o} + \{\frac{P(x)}{P_o}\}^2\right]^2 + \left[\frac{V(x)}{V_o}\right]^2 \leq 1.0 \tag{14}$$

where, M_o ($=f_y D^3/6$), P_o ($=A_s f_y$) and V_o ($=A_s f_y / \sqrt{3}$) are the ultimate moment, axial force and shear force, respectively, under non interactive stress conditions. Under any combination of the interacting stresses, $\lambda(x)$ equaling unity implies the ultimate bar axial stress.

5. VERIFICATION OF BOND STRESS-STRAIN-COUPLED SLIP MODEL

5.1 CURVATURE-SHEAR SLIP RELATION

Since the basic compatibility proposal in the model relates the curvature distribution with the shear slip of the reinforcement, the comparison of experimentally measured and computed shear slips of bar (from Eqn. 4) using the experimental obtained maximum bar curvature, is shown in Fig. (4), for some typical specimens. Satisfactory correlations can be observed.

5.2 STEEL STRESS-PULLOUT RELATION AT INTERFACE

Verification of the bar stiffness and strength is done by testing reinforced crack and joint planes, as explained in the test setup, which introduces the coupled displacement path for the embedded bar. Testing was carried out for different shear plane geometrical types (processed, P, and unprocessed, U, construction joints, CJ, and rough cracks, RC) and material properties (normal concrete, NC and High Performance Concrete, HPC), along with different reinforcement ratios. These define unique coupled displacement paths according to the equilibrium and compatibility conditions at the interface. The test and computed steel axial mean stress versus the pullout and associated transverse shear slip at the interface are shown in Figs. (5a to g). The mean axial stress versus strain

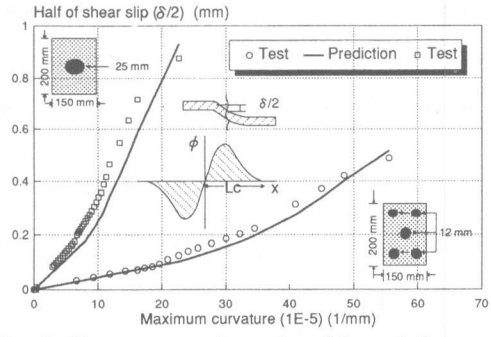

Fig. 4: Curvature vs. shear slip of bar relation

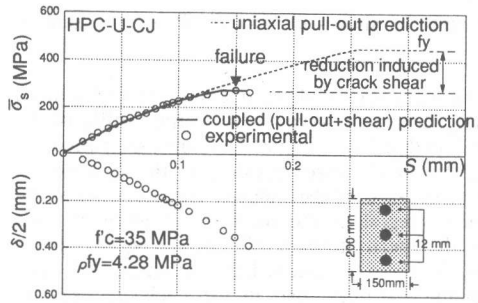

Fig. 5(a): Specimen 1

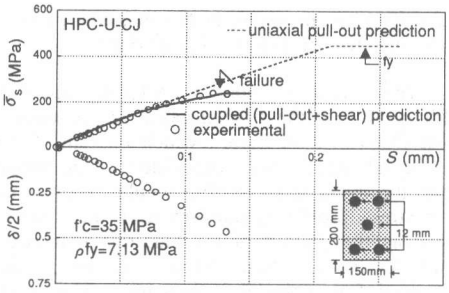

Fig. 5(b): Specimen 2

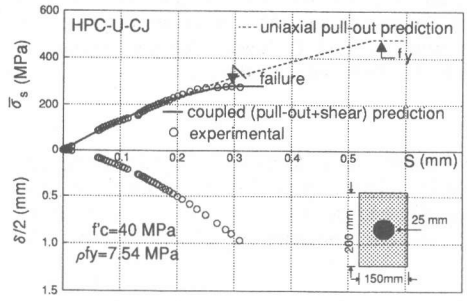

Fig. 5(c): Specimen 3

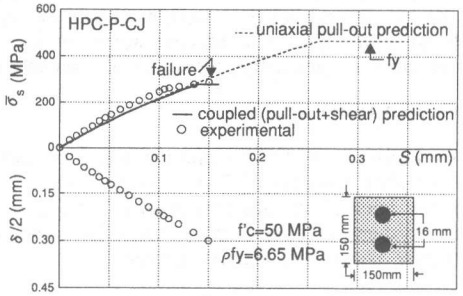

Fig. 5(d): Specimen 4

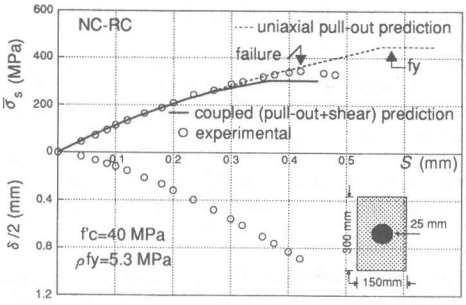

Fig. 5(e): Specimen 5

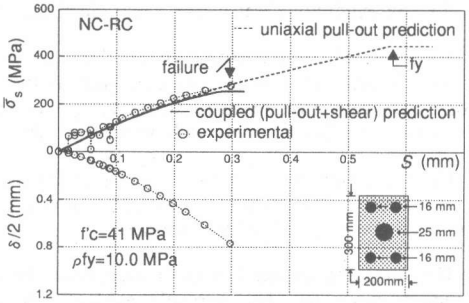

Fig. 5(f): Specimen 6

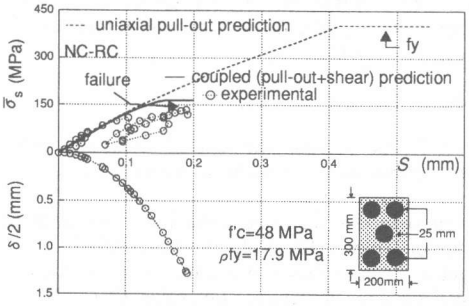

Fig. 5(g): Specimen 7

Fig. 5: Mean axial stress relation with pullout and associated transverse slip at interface

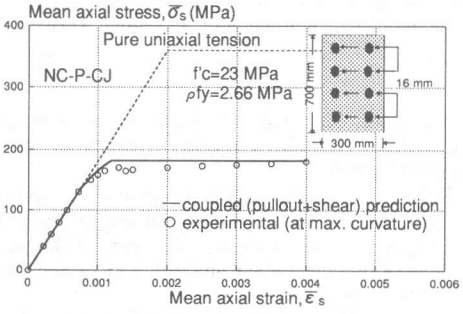

Fig. 6: Mean axial stress and strain at maximum curvature location of bar (Specimen 8)

results for one specimen, at the maximum curvature location, is shown in Fig. (6). Pure axial pullout results are also shown for comparison.

The satisfactory correlation for the initial part of the steel stress-pullout relation, before localized yielding, verifies the first proposal of the model regarding the quantitative effect of the profile of the '*Bond Deterioration Zone*', which explains the increased pullout, as compared to uniaxial pullout of the original model with bond deterioration suppressed. After the localized yielding of the extreme bar fibers, the mean strain profile would become nonuniform, because of the induced curvature, since the mean stress profile is uniform near the crack. Since the integral of the mean strain along the bar represents the pullout of the bar, this nonuniformity in the mean strain profile would be the source of the additional pullout, for a given mean stress level, observed in coupled displacement path tests as compared to uniaxial pullout tests. The prediction of the non-linear part in the steel stress-pullout relation verifies the second proposal in the model regarding the quantitative effect of the '*Curvature Influencing Zone*'. By consideration of the limiting value of the interactive stresses possible at the maximum curvature location, due to combined axial and bending stresses, the ultimate axial force of the bar can be predicted as well, as shown in Figs. (5 and 6). In general, the steeper the displacement path, in terms of δ_b / S, brought about by increased reinforcement ratio, lower concrete strength or flatter interface geometry, the lower the mean axial stress, $\overline{\sigma}_s$, that can be attained.

6. CONCLUSIONS

1) By utilizing two basic proposals, based on experimental results, of a '*Bond Deterioration Zone*' and a '*Curvature Influencing Zone*', coupled with a compatibility relation to predict curvature from shear slip, the internal stresses and strains (both along the bar axis and across its section) along with the entire system of forces acting on a bar embedded in concrete, subjected to coupled pullout and transverse shear slip, can be computed.

2) The compatibility relation between bar curvature and the normal displacement of the bar can be established using the Euler-Kirchoff hypothesis of plane sections, and is verified with experimental results, by predicting transverse shear displacement of the bar from its curvature distribution.

3) The reduced axial stiffness of the bar can be computed from the initiation of localized plasticity in the reinforcement inside concrete, even as the section at the interface is in purely elastic state. The progressive reduction of axial stiffness, due to gradually increasing plasticity both along the bar axis and across the bar section, with increasing shear displacement, can be predicted for test data.

4) The maximum axial confining stress attained in the reinforcement at the interface can be predicted by considering the ultimate interactive stress possible at the maximum curvature location, due to combined axial and bending stresses.

5) The proposed model has been independently verified when coupled displacement paths is used as an input parameter. For versatile applicability the prediction of stress transfer behavior of a RC interface, by combining with an aggregate interlock model, needs to be established. A supplementary feature of the proposed model is the evaluation of shear force acting on the bar at the crack, i.e. dowel shear, which can be added to the aggregate interlock model to obtain the total shear transferred at the interface, without any additional superpositional considerations.

REFERENCES

1) Maekawa, K., Mishima, T., Khan, J. and Qureshi, J.: Reduced axial stiffness of deformed bars under shear slip along crack in concrete, submitted for publication to CEB conference,'Bond in Concrete', 1993.
2) Shima, H., Chou, L. and Okamura, H.: Micro and macro model for bond behavior in reinforced concrete, Journal of the faculty of engineering, University of Tokyo (B), Vol. 39, No.2, 1987.
3) Bujadham, B., Maekawa, K. and Mishima, T.: Cyclic discrete crack modelling for reinforced concrete, Computer aided analysis and design of reinforced concrete structures, Pineridge Press, 1990, pp. 1225-1236.
4) Mishima, T., Yamada, K., and Maekawa, K.: Localized deformational behavior of a crack in RC plates subjected to reversed cyclic loads, Proc. of JSCE, No. 442/V-16, Feb., 1992, pp.161-170.